MODEL CALCULATION OF THE SCANNED FIELD ENHANCEMENT FACTOR OF HEMISPHERICAL CNT TIP

A Dissertation on Submitted in the partial fulfillment of the requirements of the degree of

MASTER OF TECHNOLOGY

In

NANO SCIENCE & TECHNOLOGY

By

SHUBHENDU SACHIN

2K14/NST/16

Under the Guidance of

Prof. Suresh C. Sharma
HOD, Applied Physics
DTU, New Delhi

Department of Applied Physics,
Delhi Technological University
(Formerly Delhi college of Engineering)
Govt. of NCT of Delhi
Main Bawana Road, Delhi-110042
JUNE 2016

Department of Applied Physics
Delhi Technological University (DTU)
(Formerly Delhi College of Engineering, DCE)
Govt. of NCT of Delhi
Bawana Road, Delhi-110042

CERTIFICATE

*This is to certify that the Major project report entitled "***MODEL CALCULATION OF THE SCANNED FIELD ENHANCEMENT FACTOR OF HEMISPHERICAL CNT TIP***" is a bonafide work carried out by* **Mr. Shubhendu Sachin** *bearing Roll No.* **2K14/NST/16**, *a student of Delhi Technological University, in partial fulfilment of the requirements for the award of Degree in* **Master of Technology** *in* "**Nano Science & Technology**". *As per declaration of the student this work has not been submitted to any university/institute for the award of any degree/diploma.*

(**Professor S. C. Sharma**)
Supervisor
HOD, Applied Physics
Delhi Technological University,
New Delhi 110042

Candidate Declaration

I, hereby, declare that the work which is being presented in this thesis entitled "**MODEL CALCULATION OF THE SCANNED FIELD ENHANCEMENT FACTOR OF HEMISPHERICAL CNT TIP**" is my own work carried out under the guidance of Prof. Suresh C. Sharma, Head of Department, Department of Applied Physics, Delhi Technological University, Delhi. I further declare that the matter embodied in this thesis has not been submitted for the award of any other degree or diploma.

Date: Shubhendu Sachin

Place: New Delhi 2K14/NST/16

Acknowledgement

First and foremost I would like to thank my parents for their blessings, support and guidance throughout my academic career.

I sincerely thank my supervisor **Professor S. C. Sharma,** Head of Department, Applied Physics, Delhi Technological University for all his support and guidance. His calm attitude and simple nature has always motivated me to how to do any work.

I am also thankful to Ms. Aarti Tiwari, Mr. Ravi Gupta and Ms. Neha Gupta (Research scholars) for their valuable support and guidance in carrying out this project.

I deeply grateful to Dr. M. S. Mehta (Branch coordinator, NST), Assistant Professor, Applied Physics for his support and encouragement in carrying out this project.

I express my sincere gratitude to all the faculty of Department of Applied Physics. Their moral support and encouragement has played an important part in completion of my master's degree.

I thank all my friends to keep me cheerful and make me smile whenever I feel low.

Shubhendu Sachin

2K14/NST/16

Dedicated to my parents…

Table of Contents

List of tables

List of figures

ABSTRACT

To examine the field enhancement factor for conducting hemispherical carbon nanotube (CNT) tip between two parallel plates. Hemispherical CNT tip is more realistic than floating sphere. To get the more accurate value of field emission and the screening effect of the cluster of hemispherical CNTs tip, the electrostatic potential for hemispherical CNT has been derived. Using mirror image method as Ahmed et al.[5] and Wang et al. have used to calculate field enhancement factor and screening effect of array of CNTs by considering floating sphere for any positional distribution of CNTs. The nature of electrostatic potential decreases with increase in radial distance as a point charge. We have derived an expression for field enhancement factor for individual hemispherical CNT tip. The screening effect for cluster of CNTs for any positional distribution dependence on the length of the CNT and the spacing between the CNTs is shown. Then compare the proposed model with experimental result of CNT with hemispherical tip.

CHAPTER 1: Introduction to Carbon Nanotube

1.1 Introduction

Materials have been of great interest to human beings since immemorial. a few years ago it was found that we can use rocks to break things which we can't break with our bare hands. than it was found that if a rock containing copper was placed on a fire, molten copper could be collected. this discovery lead us to production of metals from metal ores. in this way civilization keeps on changing from stone age to bronze age and then iron age. the current age of silicon and other advanced materials. the coming age will be dominated by nanotechnology or we can say nano age[1].

New technologies requires new materials which is provided us by materials science and engineering. microstructural engineering has helped us a lot in understanding the structure of materials. the unique properties of materials due to ultrafine particle sizes were recognized early in the 20th century. the classic lecture by Richard P Feynman titled "There's plenty of room at the bottom", on 29 December 1959, at the annual meeting of the American Physical Society, opened up a whole new field which was known as 'nanotechnology'[1].

The word 'nano' is derived from a Greek word means dwarf. mathematically nano is one billionth (10^{-9}) of a unit. Exact definition for nano can't be defined. so we can say nanomaterials can be those materials which have at least one of their dimensions in the nanometric range, below which there is significant variation in the property of interest compared to microcrystalline materials[1].

According to Siegel nanostructured materials can be classified into four categories according to their dimensionality: 0D: nanoclusters, 1D: multilayers, 2D:nanograined layers and 3D: equiaxed bulk solids. All these are shown in fig. 1.1

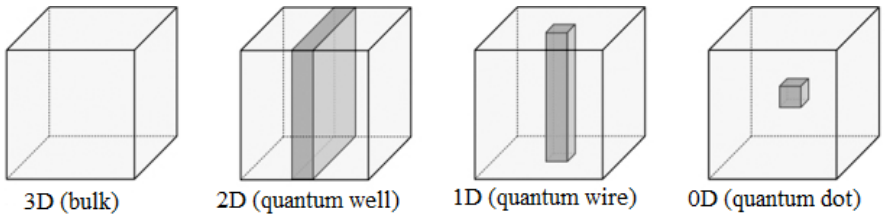

Figure 1.1 Schematic diagram of confinement in quantum well, quantum wire and quantum dot.

Nanostructures materials fascinates us as it may occur in several different geometric configurations including rods, tubes, wires horns, shells, pores, etc. They have unique properties and are developed for specific applications. Some famous and mostly used nanostructures are nanowires, nanorods, nanoshells, nanotubes and nanofluids. As we are using nanotubes in this project work so let's have a brief introduction about nanotubes. These

are tubes which have their diameters in the nanoscale. Mostly used nanotubes are carbon nanotubes. These are alltropic form of carbon and other allotropes of carbon are graphit, amorphous carbon, diamond, carbon cluster like C_{60}, C_{70} etc[2] as shown in figure 1.2.

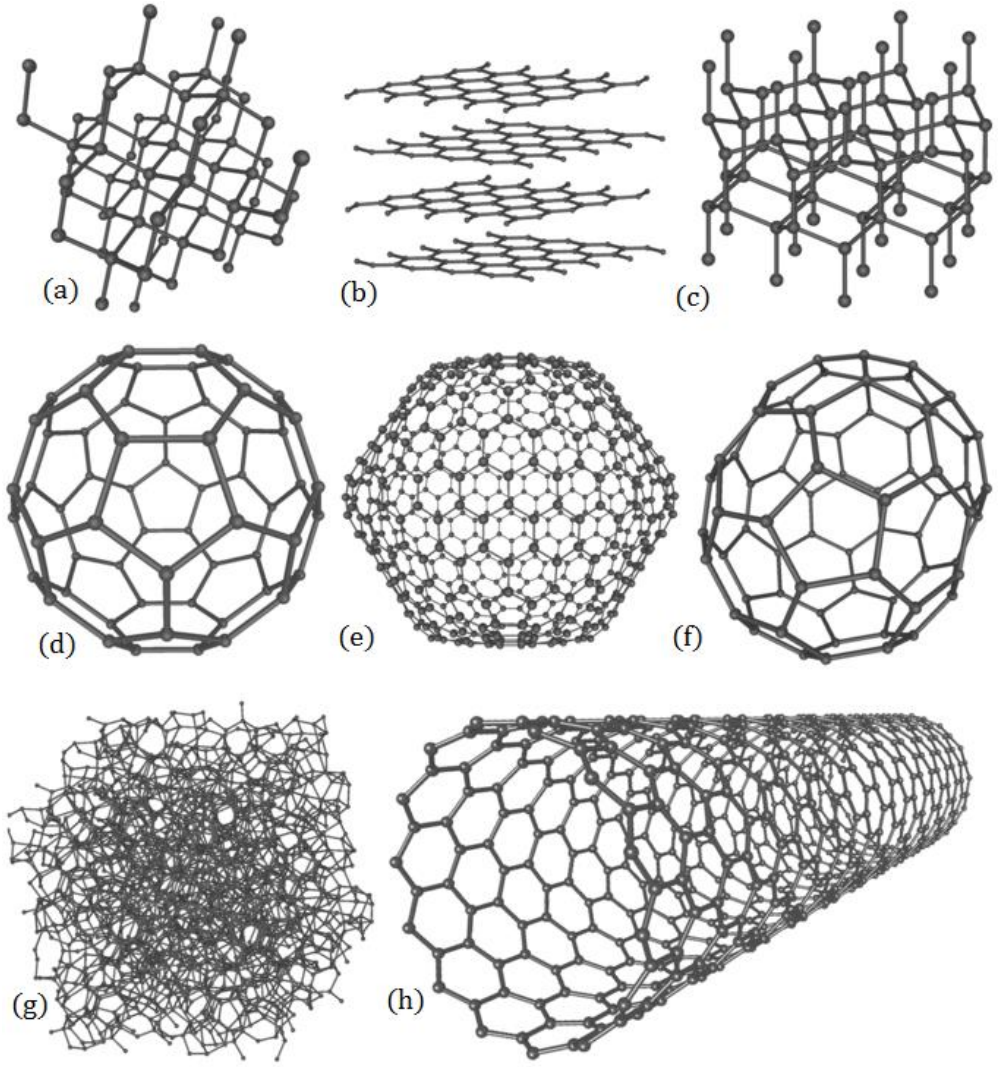

Figure 1.2 Allotropes of carbon: (a) Diamond, (b) Graphite, (c) Lonsdaleite, (d) C60 (Buckminsterfullerene), (e) C540 (see fullerene), (f) C70 (see fullerene), (g) Amorphous carbon, (h) Singled-walled carbon nanotube.

They exhibit different properties due to different bonding and structures. There are two hybridization states of carbon i.e. sp^2 and sp^3. Graphite, carbon clusters and CNT are sp^2 hybridized and diamonds are sp^3 hybridized. Graphite and carbon cluster are of same hybridization but atoms arrangement in both are different i.e. in graphite atoms are arranged on the plane and in carbon clustaers like C_{60}, C_{70} and etc. are in shape of football i.e. in case of C_{60} we called it fullerenes which were discoverd by Rick Smalley and co-workers in 1985[2].

There are different types of CNT, Single walled nanotubes and Multi walled nanotubes, their

length to diameter ratio exceeds nearly 10,000. At the end of these nanotubes half fullerene molecules is capped. Bacon originally proposed that nanotubes are graphene sheet rolled like a scroll but it was Ijima who first determine that nanotubes were concentrically rolled graphene sheets with a large number of potential helicities and chiralities[2].

1.2 Single-walled nanotube (SWNT)

These nanotubes have diameter about 1 nanometer and their tube length can be thousands time longer and length up to centimeters have been produced. These exhibit electric properties which are different from MWNT. SWNT can help in miniatirsing electronics beyond MEMS[2].

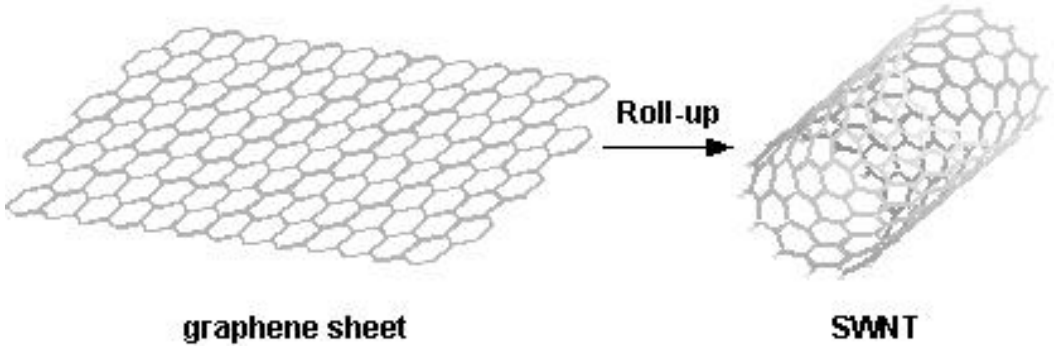

Figure 1.3 SWNT made by rolling of graphene sheet.

1.3 Multi-walled nanotube (MWNT)

These are made up of multiple layer of graphite rolled on themselves to form a tube or in other words these tubes made of number of concentric tubes. These concentric layer may be identical or not in terms of chirality[2].

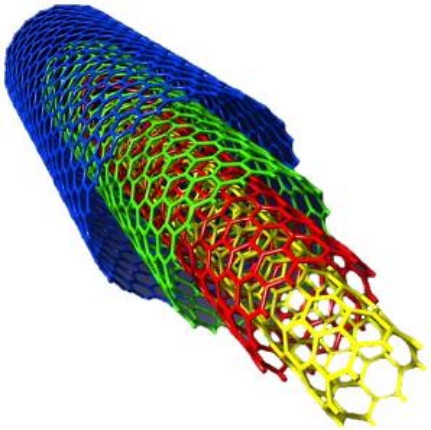

Figure 1.4 Multi walled carbon nanotube.

1.4 Chirality

Nanotubes are also classified as armchair, zigzag and chiral tubes depending on their chirality. chirality of the tube defined by chiral vector whose equation is $C_h = n\,a_1 + m\,a_2$, where n and m are integers, $a_1$and a_2 are basic vectors of hexagonal lattice, C_h is the rolling vector about which graphene sheet has to roll to get CNT and θ is rolling angle [2] as shown in figure 1.5.

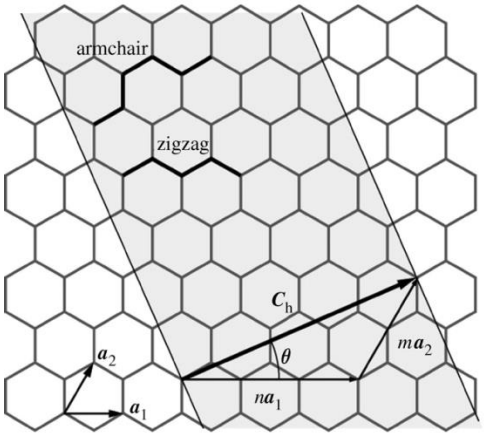

Figure 1.5 schematic diagram of formation of different types of CNT.

For armchair nanotubes, the armchair vector divides the hexagon into half i.e. the armchair vector coincides with rolling vector, hence rolling vector will become $C_h = n\,(a_1 + a_2)$, i.e. n = m.

For Zigzag nanotubes, the rolling angle is equal to 30^0, i.e. rolling vector will become $C_h = n\,a_1$, where m = 0.

For Chiral nanotubes, the rolling angle must be in between 0^0 to 30^0 then, rolling vector wiil become $C_h = n\,a_1 + m\,a_2$, where m≠ n. m and n values gives the chirality or twist of the CNT, values of m and n decides whether single walled CNT is metallic or semiconducting. Each CNT is capped with some fullerene caps, as shown in figure

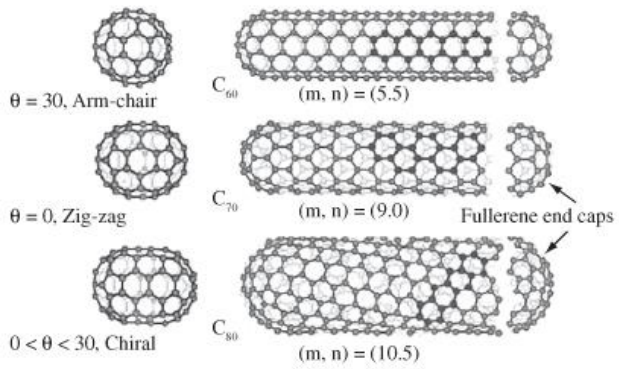

Figure 1.6 Different types of CNT with their different end caps.

In general we found that, the armchair nanotubes are metallic in nature, the chiral nanotubes are low conducting or semiconducting in nature and the zigzag nanotubes have small bandgap and due to this its nature varies from semi metallic to semi conducting.

Figure 1.7 Different types of CNT and their properties.

1.5 Properties of CNT

1.5.1 Mechanical properties

Carbon nanotubes have high tensile strength and elastic modulus in other words they are the strongest and stiffest materials. The strength in these tubes are due to covalent sp^2 bonds formed between carbon atoms. On high tensile strain, the tubes experienced plastic deformation and this deformation is permanent. This deformation starts at strains of nearly 5% and releases strain energy at maximum strain before undergoing fracture.

1.5.1.1 Hardness

A single-walled carbon nanotubes can bear pressure up to 25 GPa until some [plastic/permanent] deformation is not there and then it undergoes a transformation to superhard phase nanotubes.

Although the strength of individual CNT shells is extremely high but a weak shear interactions between tube and adjacent shell lead to enough reduction in the effective strength of MWNT and CNT bundles down to only a few GPa.

CNTs are not so strong under compression because of its high aspect ratio and hollow structure, they tend to undergo buckling when placed under compressive, bending or stress torsional.

1.5.2 Thermal properties

CNTs are very good thermal conductors, they exhibit ballistic conduction property, As compared to copper, CNTs show Measurements show thermal conductivity of 3500 $W \cdot m^{-1} \cdot K^{-1}$ along its axis at room-temperature, a metal can transmits 385 $W \cdot m^{-1} \cdot K^{-1}$ which is known for good thermal conductivity.

1.5.3 Electrical properties

Electrical properties depend upon the chirality of the CNTs which we have discussed earlier. CNTs with small diameter can influence electrical properties. Theoretically, electric current density of 4×10^9 A/cm^2 can be carried by metallic nanotubes, which is $\geq$ 1,000 those of metals such as copper.

CNTs are referred as 1D conductors because electrons can propagate only through its tube axis due to its nanoscale cross-section.

1.5.4 Field Emission

whenever a high electric field is applied on a conductor the effective energy barrier of that conductor get reduced so the electrons easily tunnel through it and get emitted from the surface of the conductor. The Field emission display works on this principle.

There are two types electron emitter, cold electron emitter and thermionic emitter. cold emission of electron is based on field emission principle and carbon nanotubes have low turn on field emission and high current density. CNTs can be used in electron microscopy because it can emit single coherent beam of electron. CNTs can be used in multiple electron beam like in flat displays.

The emitted current depends upon the work function of the emitting surface and local field on the emitting surface, this dependency can be described by Fowler-Nordhiem (F-N) model as shown in figure

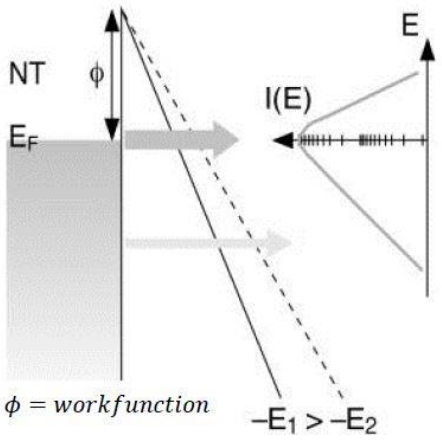

Figure 1.8 Field emission from metallic emitter.

By quantum mechanical tunnelling, the relation between emitted current density and local electric field by F-N equation

$$J = \frac{aE_t^2}{\emptyset}\exp\left(\frac{-b\emptyset^{3/2}}{E_t}\right) \quad (1)$$

where

$a = 1.56 \times 10^{-6}\, AV^{-2}\, eV,$

$b = 6.83 \times 10^{7}\, eV^{-3/2}\, cm^{-1},$

$E_t\ is\ Electric\ field\ at\ the\ tip\ ,$

$\emptyset = Work\ function$

E_t can be written as $E\beta$, E is the applied electric field, i.e., E = V/d, β is the field enhancement factor. Field enhancement factor can also be written in terms of height and the radius of the tip.

1.6 Application of CNT

1.6.1 A field emission display (FED)

it is a flat panel display that uses large area field electron emission sources to produce a color image by striking electrons on colored phosphor. These displays will consume half of the power than LCD system.

Due to field emission characteristics(i.e. low on field, high current density) of CNT, it can be

used as a electron source for field emission displays. It will reduce the manufacturing cost of field emission displays and provides enlargement in the dimensions of panels.

The CNT FED is similar to the conventional Spindt type FED. In this CNT is used as electron emitter in place of metal tip. Hence its manufacturing process is easy and low at cost. CNT FED structure is shown in figure 1.9.

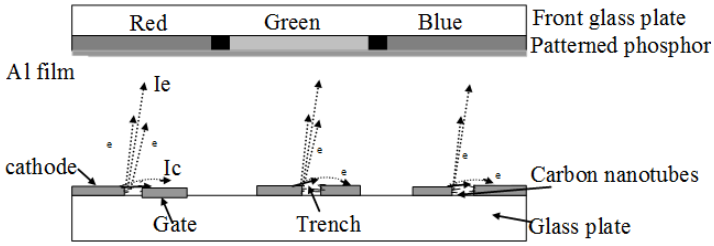

Figure 1.9 Schematic diagram of CNT FED.

1.6.2 Nanotube speakers

These are aligned CNT film which is drawn from array of CNT and have potential as thermoacoustic loudspeakers. These film have extremely low heat capacity which gives wide frequenc response range and a high level of sound pressure. These thin film loudspeakers are flrxible, transparent, magnet free and stretchable.

Figure 1.10 Thin film, flrxible, transparent, magnet free and stretchable nanotube speakers.

1.6.3 Nanotube thermocell

Thermocell are thermogalvanic cell which convert thermal energy into electrical energy by electrochemical reactions. The nanotube thermocell works on the same as conventional thermocell but in nanotube thermocell, MWNT are used as electrodes which will convert thermal energy into electrical energy three times efficiently as compared conventional one.

1.6.4 Energy Storage

1.6.4.1 Lithium batteries

CNT based lithium ion batteries can be made because CNT have highest reversible capacity, can be used as electrodes, high surface area, thermal conductivity, can be utilized as free standing CNT so that its specific energy density can be increased by 50% and these electrodes can also be used as active ion lithium storage.

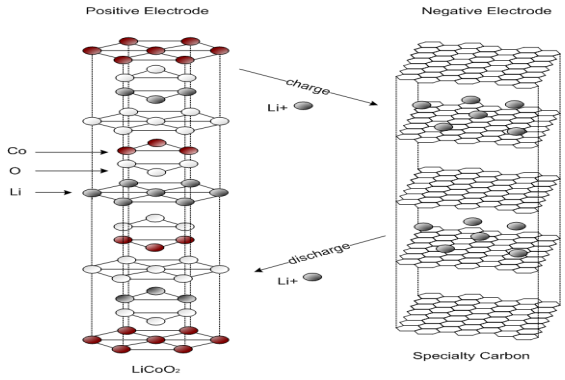

Figure 1.11 Storage of lithium in CNT

1.6.4.2 Hydrogen storage

Hydrogen is good source of energy and it can be used in future in many fields and with the help of SWNT we can store hydrogen. there are mechanism of storing hydrogen physisorption and chemisorption in CNT.

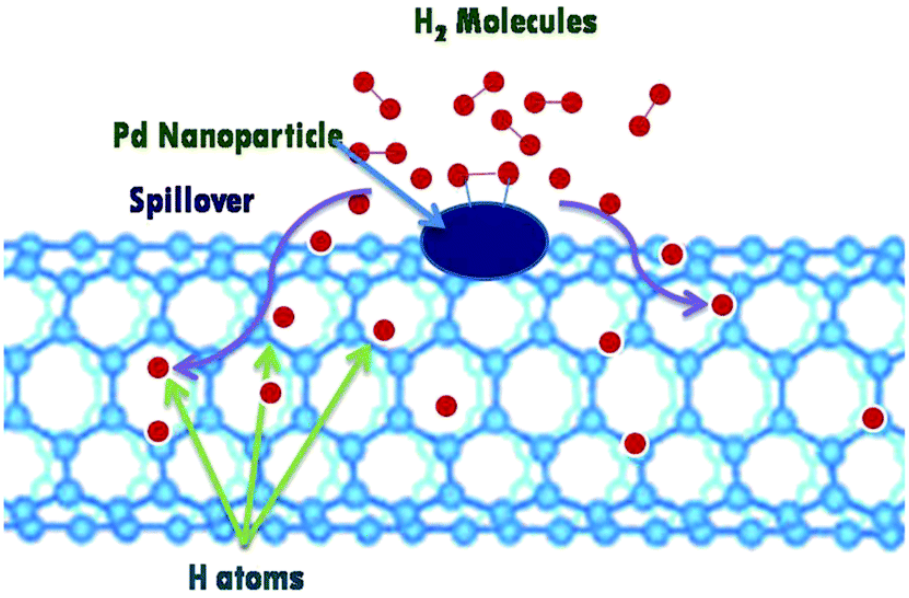

Figure 1.12 Storage of hydrogen in CNT.

1.6.5 AFM tips

CNT have many properties like high aspect ratio, excellent elastic buckling property, high Young's modulus, electrical and thermal conductivity. All these properties can be made CNT as ideal probes in AFM.

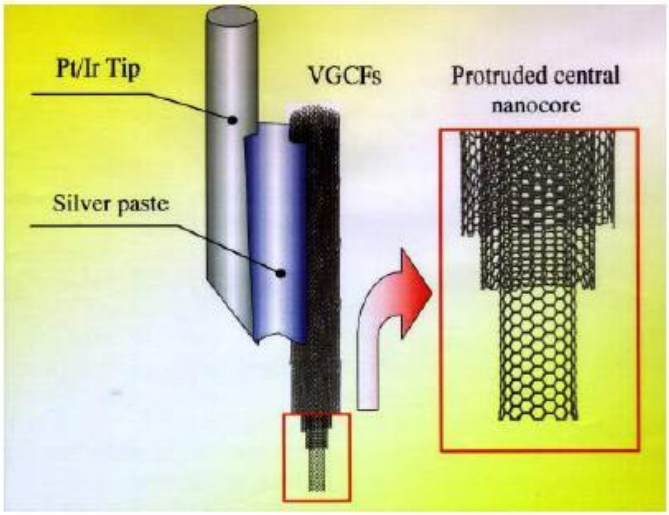

Figure 1.13 CNT probe in AFM.

1.6.6 Biological applications

1.6.6.1 DNA sequencing

Carbon nanotubes can fit in the grove of DNA strand, if we apply voltage across CNT, different current signals will appear by different DNA base pair.

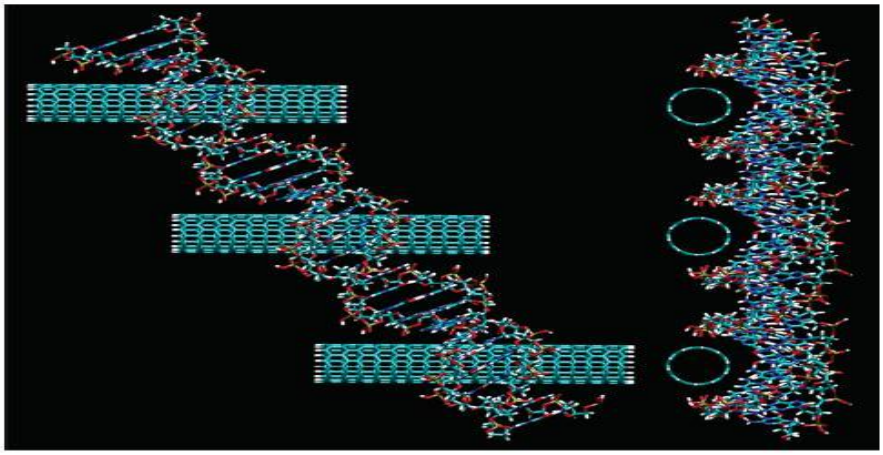

Figure 1.14 DNA sequencing with CNT.

1.6.6.2 Artificial muscles

Carbon nanotubes can used to make artificial muscle, these artificial muscles are stronger than steel and flexible than rubber. Aerogel made from CNT can electrically power these artificial muscles.when voltage is applied the sheet become 220% wider and thicker. These artificial muscles can generate 30 time and more force than human muscles.

CHAPTER 2: Literature Review

2.1 Literature review

The field enhancement factor depends upon the geometry of the CNT tip as sharper the tip of CNT as greater the value of the field enhancement factor i.e. more emission of electron will take place. According to Grigory et al[3] CNT with different tips will have different values of field enhancement factor i.e. CNT with conical tip of opening angle 30^o will have greater value than conical tip of opening angle 90^o because of its sharpness.

The change in tip of CNT shape will change the field enhancement factor by 5% - 7%. As shown in figure

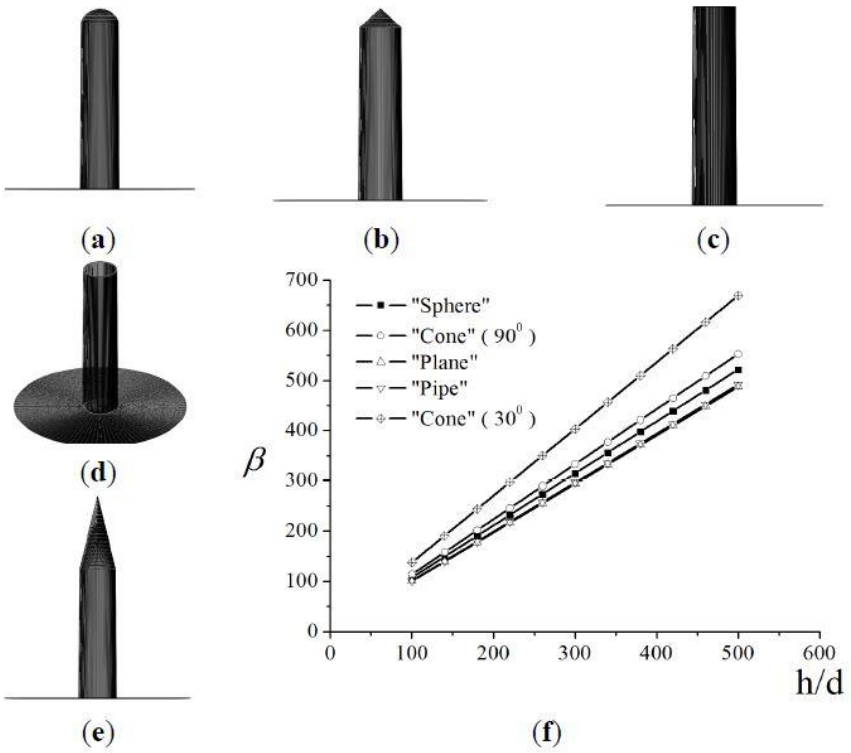

Figure 2.1 CNTs with different tips and their field enhancement factor with respect to aspect ratio.

Many authors have done work on field enhancement factor for Hemispherical CNT tip

theoretically and experimentally. Theoretically, many authors have given many expressions by considering floating sphere on emitter-plane model and some have given the expressions by taking hemisphere on a post model.

In theoretical approach, floating sphere on emitter-plane model have taken by Nicolaescu et al. [4], Ahmed et al. [5] and Utsumi et al. [6] have given the expression for field enhancement factor is

$$\beta_o = \frac{L}{\rho} + 2.5 \tag{2}$$

hence L=h+ρ

$$\beta_o = \frac{h}{\rho} + 3.5 \tag{3}$$

where L is the length of protrusion, h is the height of CNT and ρ is the radius of the CNT tip. Some authors have done the same work by considering hemisphere on a post model. which is more realistic, they have deduced many expressions, Rohrbach[7] et al have give the expression

$$\beta_o = \frac{h}{\rho} + 3 \tag{4}$$

in the limit that L$\gg \rho$, this formula become

$$\beta_o \cong \frac{L}{\rho} \tag{5}$$

it is a rough approximation and at L= ρ

$$\beta_o = 3 \tag{6}$$

Accoeding to Kokkorakis, Modino and Xanthakis (KMX)[8] and EV's[9,10] said that all these equations are over predicted the value of the apex enhancement factor β_o for hemisphere on a post model at large value of $\frac{L}{\rho}$. From EV's, the $\frac{L}{\rho}$ ratio gives appropriate values of β_o in the range $4 \leq \frac{L}{\rho} \leq 3000$ within $\pm 3\%$ by

$$\beta_o \cong 1.2(2.15 + \frac{h}{\rho})^{0.9} \quad (7)$$

and gave simpler expression suitable within the range $30 \leq \frac{L}{\rho} \leq 2000$ and valid upto $\pm 25\%$ is

$$\beta_o \cong 0.7\ \frac{L}{\rho} \quad (8)$$

for smaller values of $\frac{L}{\rho}$ equation 3 is good approximation.

According to KMX[8], the equation for field enhancement factor

$$\beta_o = 5.93 + 0.73\frac{L}{\rho} - 0.0001\frac{L}{\rho}^2 \quad (9)$$

gives appropriate result within the range $20 < \frac{L}{\rho} < 600$. Results of all equations compared in Table 1.1[11]

Table 1.1

$\frac{L}{\rho}$	Hemisphere on post model	
	Eq. 7	Eq. 9
1	3.37	6.66
1.3	3.66	6.88
2	4.32	7.39
4	6.15	8.85
11	12.2	13.9
21	20.3	21.2
31	28	28.5
101	77.9	78.6
301	205	217
601	382	409
1001	603	636

Comparison of field enhancement factor obtained by various model and approximations as a

function of $\frac{L}{\rho}$, where L is the total protrusion length and ρ is the base radius.

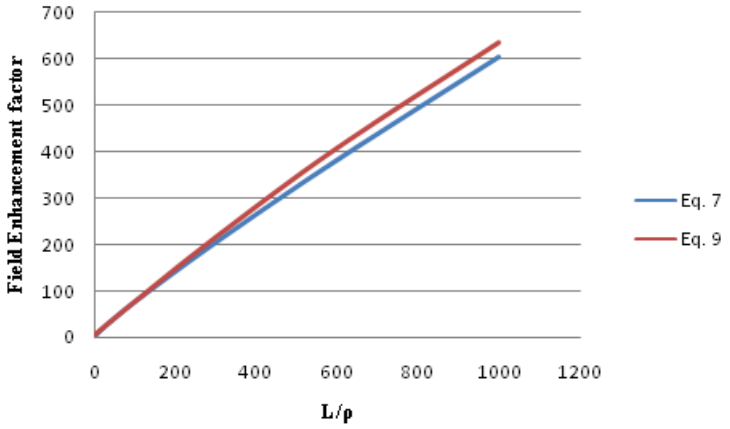

Figure 2.2 Graph between field enhancement factor and aspect ratio of Eq. 7 and Eq. 9

Wang et al has shown the field enhancement factor of hemispherical CNT tip by considering floating sphere between the parallel anode and cathode plate. They derived the formula

$$\beta_o = \frac{h}{\rho} + 3.5 \tag{10}$$

and they also derived the influence of the distance between the parallel plates. They modify the expression under anode cathode distance influence,

$$\beta_o = \frac{h}{\rho} + 3.5 + \mathrm{A}(h/d)^3 \tag{11}$$

where A is the constant.

They conclude that the threshold voltage can be lower to some extent by decreasing the distance between the plates. The high aspect ratio and the lower distance between the plates are the main factors for strong field at apex.

Ahmed at el[5] have also derived an expression field enhancement factor under any positional distribution and for screening effect of the CNT by taking same model of wang et al. They derived an expression for screening effect of array of CNT

$$\beta = \beta_0 - 4\left(\sum_{n=1}^{m} \frac{\frac{h}{s}}{(a^2+b^2)^{\frac{1}{2}}} - \sum_{n=1}^{m} \frac{\frac{h}{s}}{\sqrt{a^2+b^2+\left(2\frac{h}{s}\right)^2}}\right) \tag{12}$$

Theoretically, the field enhancement factor for CNT placed in cluster is smaller than isolated because of the screening effect by the neighbouring CNT. And the screening effect depend

upon the length of CNT and spacing between the CNTs. They obtain

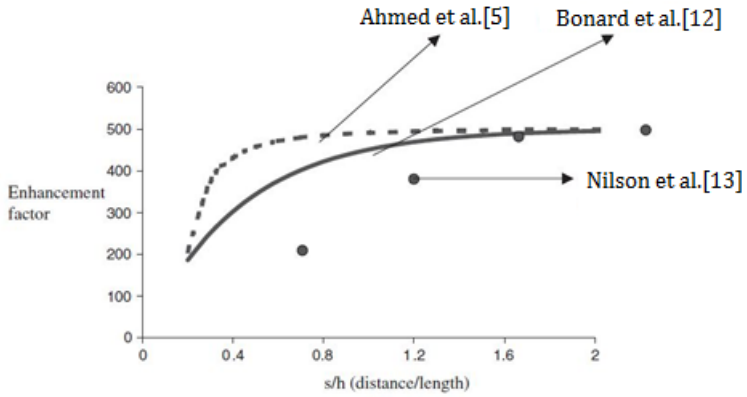

Figure 2.3 Field enhancement factor vs spacing distance 's ' obtained by Ahmed et al.[5] compared with experimental results of Bonard et al.[12] and Nilson et al.[13].

In this graph as we increase the spacing between the CNTs and length of the CNT remain constant, the field enhancement factor first increases then become constant.

Next graph, the flied enhancement factor of CNT affected by length of the CNT. In this the spacing between the CNTs remain constant and the length of the CNT changes. The same behaviour is also obtained by suh et al that the field enhancement factor first increases then after a certain value the field enhancement factor decreases due to screening effect.

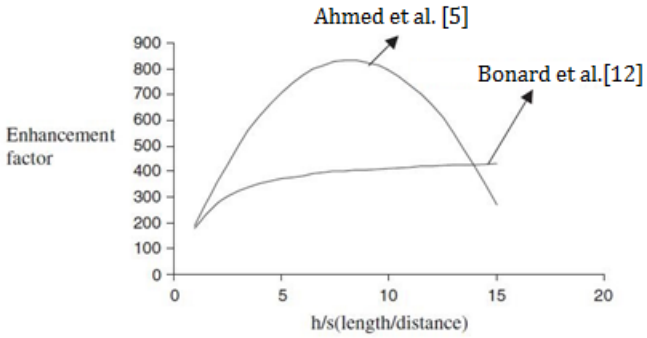

Figure 2.4 Field enhancement factor vs length ' h' obtained by Ahmed et al.[5] compared with experimental results of Bonard et al.[12].

CHAPTER 3: An Electrostatic Model for Scanned Field Emission

3.1 Introduction

Field emission of electron from CNT depends upon the geometry of the CNT tip as we have discussed in chapter 2. Early theoretical work on the field emission is done by considering floating sphere Wang et al[14] and Ahmed et al.[5]. The hemisphere on the post model is more realistic than floating sphere and we are deriving a expression for more realistic model.

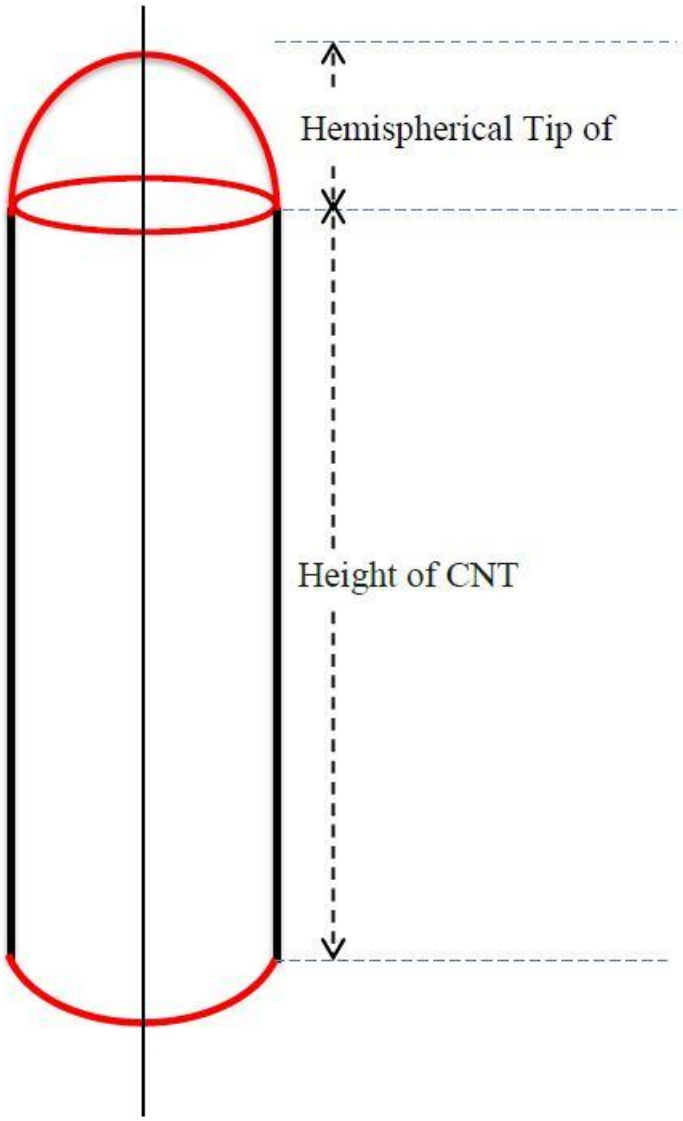

Figure 3.1 Schematic diagram of CNT with hemispherical tip.

3.2 Model

We are considering image charge effect as Wang et al[14] has done. First we have to derive expression of potential using Fredy et al[15] and Indrek[16] method, but we have to derive an expression for any arbitrary point on vacuum space so that we can study the screening effect for any positional distribution of the hemispherical CNT tip. Fredy et al[15] and Indrek have derived the expression for off axis electric field of uniformly charged ring using this method we derived for hemispherical CNT tip.

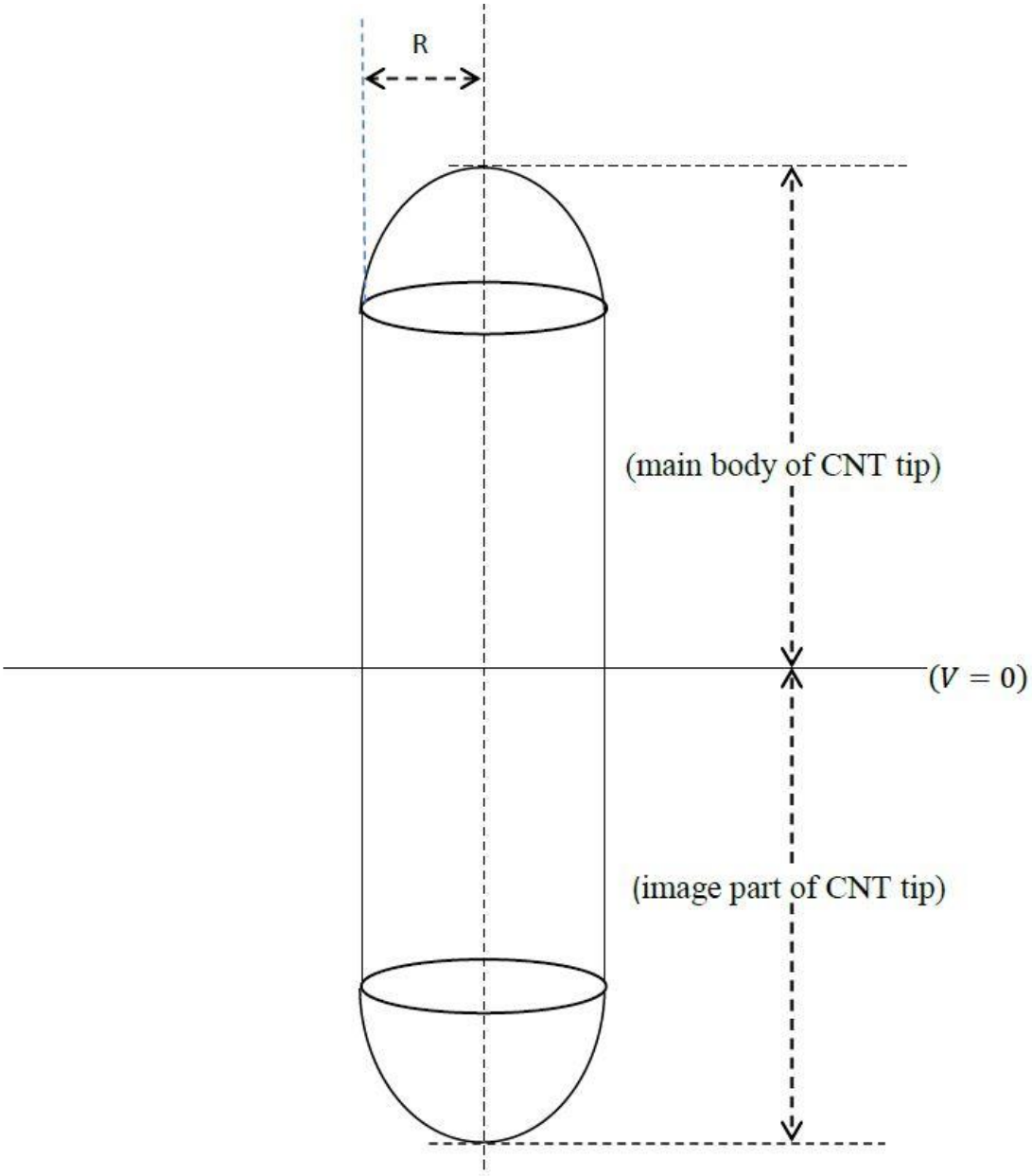

Figure 3.2 Schematic diagram of CNT and its image part.

3.3 Calculation for electrostatic potential of hemispherical CNT tip

We have derived an expression to compute the field enhancement factor of CNT under

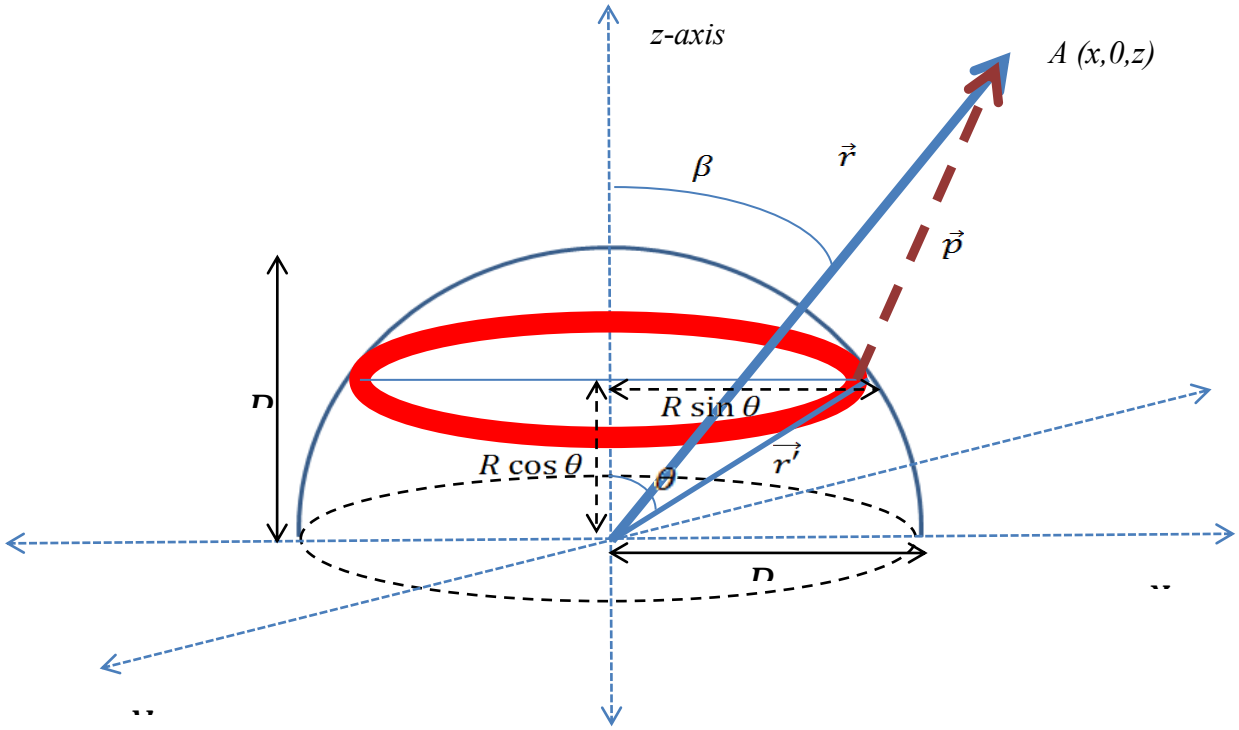

Figure: 3.3 schematic diagram of hemispherical CNT tip

any positional distribution of CNTs using a model of a floating hemisphere between parallel anode and cathode plates. An expression of potential due to charged hemisphere at any point in the space to be derived. An expression of Field enhancement factor to be derived. We are considering tip of the CNTs is uniformly charged i.e., Q and surface charge density of the tip is σ. For potential of hemispherical CNT tip, we are considering hemisphere of radius R, base of the tip in on the x-y plane as shown in figure 3.3. The curvature of the tip is along z-axis. Taking point A located anywhere in space. Due to axial symmetry, we do not lose generality by calculating potential at point A(x,0,z). Considering the hemisphere is made from infinitesimal ring charge. As shown in figure 3.4.

Consider a infinitesimal ring charge of strip width dθ at an angle θ is along z axis.

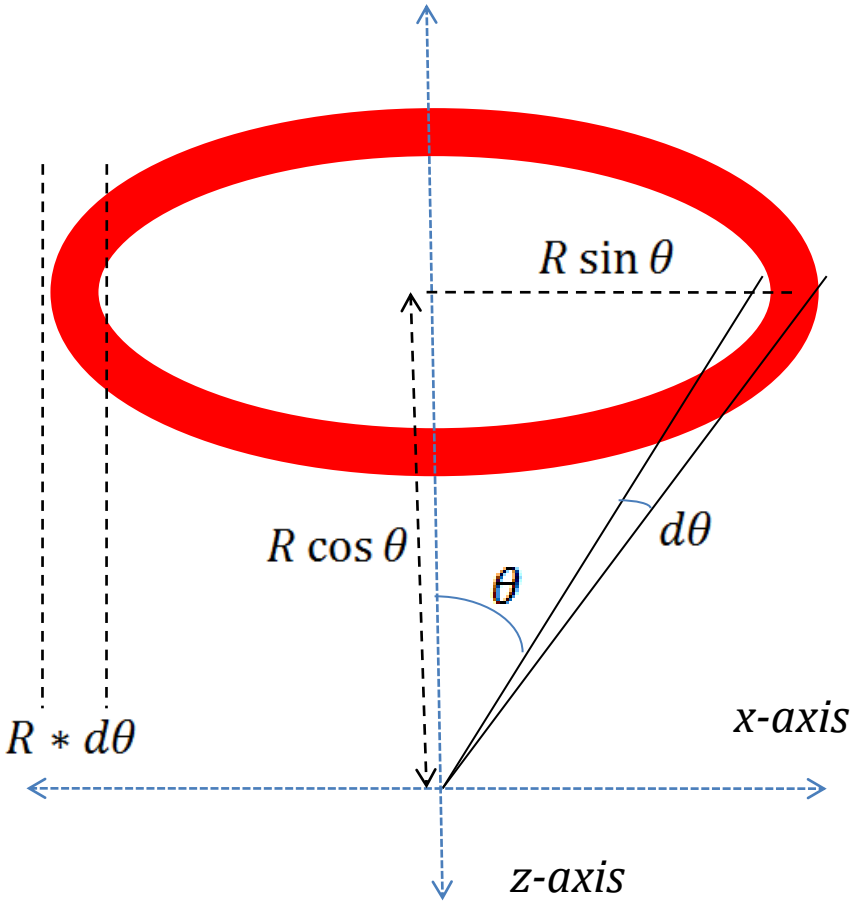

Figure 3.4 Ring element of hemispherical CNT tip

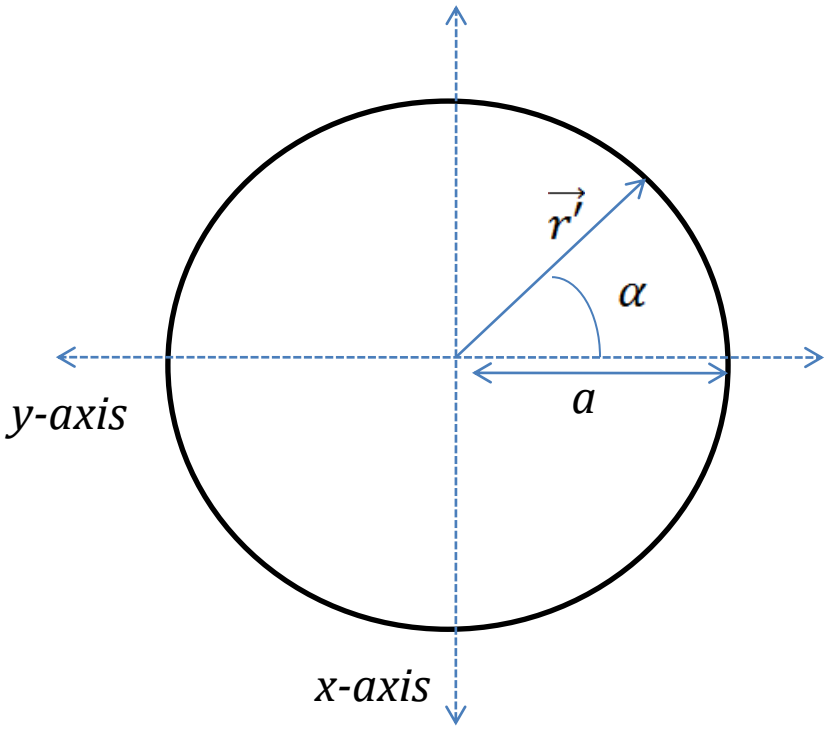

Figure 3.5 Base of the ring on XY plane.

Base of the ring is along x-y plane with radius $R \sin\theta$. Radius vector $\vec{r'}$ is moving along x-y

plane having angle α.

$$\vec{r} = x\,\hat{\imath} + z\,\hat{k} \tag{13}$$

$$x = |\vec{r}|\sin\beta \tag{14}$$

$$z = |\vec{r}|\cos\beta \tag{15}$$

$$\vec{r'} = R\sin\theta\cos\alpha\,\hat{\imath} + R\sin\theta\sin\alpha\,\hat{\jmath} + R\cos\theta\,\hat{k} \tag{16}$$

Differential charge will be

$$dq = R^2\sin\theta\, Rd\theta\, d\alpha \tag{17}$$

$$|\vec{p}| = |\vec{r} - \vec{r'}| = \sqrt{(x - Rsin\theta cos\alpha)^2 + (Rsin\theta sin\alpha)^2 + (z - R\cos\theta)^2} \tag{18}$$

Then, Potential for hemispherical CNT tip will be

$$dV = \frac{1}{4\pi\varepsilon o}\frac{dq}{|\vec{p}|} \tag{19}$$

$$dV = \frac{\sigma}{4\pi\varepsilon_0}\frac{R^2 sin\theta d\theta\, d\alpha}{\sqrt{r^2 + R^2 - (2xRsin\theta cos\alpha) - (2zRcos\theta)}} \tag{20}$$

$$dV = \frac{\sigma}{4\pi\varepsilon_0}\frac{R^2}{r}\frac{sin\theta d\theta d\alpha}{\sqrt{1 + (\frac{R}{r})^2 - \frac{2xRsin\theta cos\alpha}{r^2} - \frac{2zRcos\theta}{r^2}}} \tag{21}$$

$$dV = \frac{\sigma}{4\pi\varepsilon_0}\frac{R^2}{r}\frac{sin\theta d\theta d\alpha}{\sqrt{1 + (\frac{R}{r})^2 - \frac{2R\,sin\beta sin\theta cos\alpha}{r} - \frac{2R\,\cos\beta\,cos\theta}{r}}} \tag{22}$$

As we know that the radius of the cone is in the nanometer and radial distance is in micro meter, hence the ratio of both will be approximately equals to 0.001, which can be neglected. Using this condition we have three cases mentioned below;

Case 1: Excluding all powers of R/r

$$dV = \frac{\sigma}{4\pi\varepsilon_0 r}\frac{R^2 sin\theta d\theta d\alpha}{\sqrt{1+0+0}} \tag{23}$$

$$dV = \frac{\sigma}{4\pi\varepsilon_0 r}\frac{R^2 sin\theta d\theta d\alpha}{1} \tag{24}$$

On Integrating

$$\int dV = \frac{\sigma R^2}{4\pi\varepsilon_0 r}\int_0^{\pi/2}\int_0^{2\pi} sin\theta d\theta d\alpha \tag{25}$$

$$V = \frac{R^2}{4\pi\varepsilon_0 r}\frac{q}{2\pi R^2} \tag{26}$$

Since

$$\sigma = \frac{q}{2\pi R^2} \tag{27}$$

$$V = \frac{q}{4\pi\varepsilon_0 r} \tag{28}$$

This potential expression is similar to the potential of sphere or a charged particle, hence this expression will be invalid for hemispherical CNT tip.

Case 2: Binomial Expansion and excluding higher powers of R/r

$$dV = \frac{\sigma}{4\pi\varepsilon_0 r}\frac{R^2 sin\theta d\theta d\alpha}{\sqrt{1-\frac{2R\ sin\beta sin\theta cos\alpha}{r}-\frac{2R\ \cos\beta\ cos\theta}{r}}} \tag{29}$$

$$dV = \frac{\sigma}{4\pi\varepsilon 0 r}\frac{R^2 sin\theta d\theta d\alpha}{\sqrt{1-\frac{2R\ sin\beta sin\theta cos\alpha}{r}-\frac{2R\ \cos\beta\ cos\theta}{r}}} \tag{30}$$

$$dV = \frac{\sigma}{4\pi\varepsilon_0 r} R^2 sin\theta (1 + \frac{R\ sin\beta sin\theta cos\alpha}{r} + \frac{R\ \cos\beta\ cos\theta}{r})\ d\theta d\alpha \quad (31)$$

$$dV = \frac{\sigma R^2}{4\pi\varepsilon_0 r} (sin\theta + \frac{R\ sin\beta (sin\theta)^2 cos\alpha}{r} + \frac{R\ \cos\beta\ cos\theta sin\theta}{r})\ d\theta\ d\alpha \quad (32)$$

On Integrating both sides

$$V = \int_0^{2\pi} \int_0^{\frac{\pi}{2}} \frac{\sigma R^2}{4\pi\varepsilon_0 r} (sin\theta + \frac{R\ sin\beta (sin\theta)^2 cos\alpha}{r} + \frac{R\ \cos\beta\ cos\theta sin\theta}{r})\ d\theta\ d\alpha \quad (33)$$

For case 2, we can see that the graph is decreasing with increase in radial distance. Hence, we can say that this expression will be possible expression for our further study. Using this equation, we have derived the Field enhancement factor for CNT with hemispherical CNT tip.

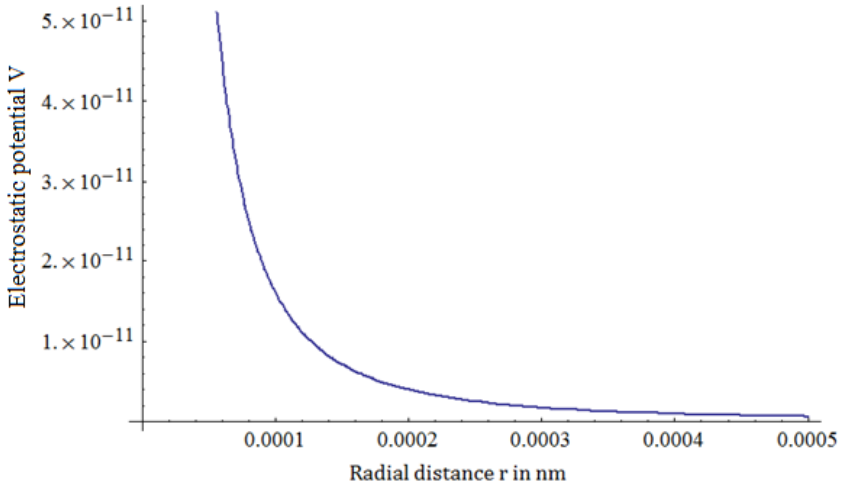

Figure 3.6 Electrostatic potential vs radial distance.

At $\cos\theta = 0$ i.e electrostatic potential at z axis will be

$$V = \frac{Q}{4\varepsilon_0 \pi r} [1 + \frac{R}{2r}] \quad (36)$$

3.4 Field enhancement factor of a hemispherical CNT tip

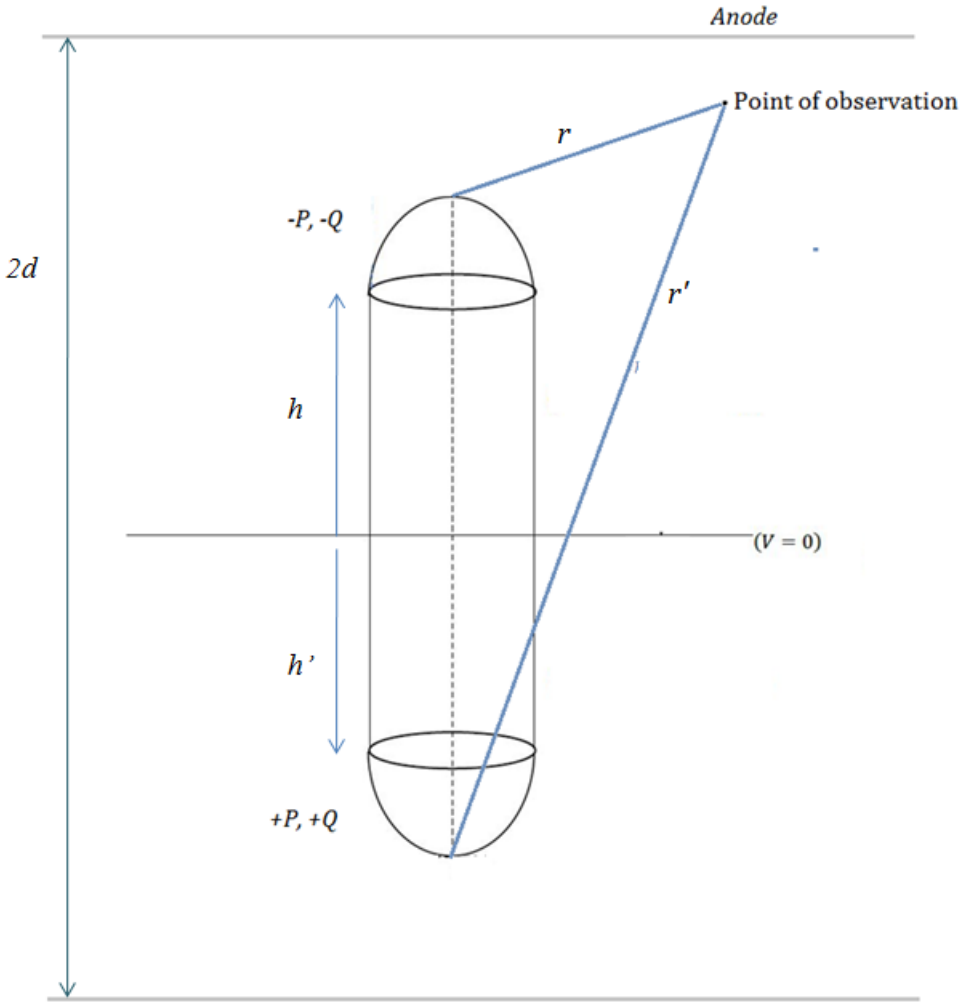

Figure 3.7 Model of hemispherical CNT tip with its mirror image part.

Dipole -P and -Q is charge on the hemispherical CNT tip and +P dipole and +Q charge is on the image part o the hemispherical CNT tip. CN is placed between the anode cathode plates which is 2d distant apart. Image part of CNT makes the cathode plate at zero potential. Voltage V_a is applied between the plates. Point of observation is in the space having spherical coordinates of (r, θ). Hence the potential at point of observation will be

$$\emptyset(r,\theta) = \frac{1}{4\pi\varepsilon_0}\left[\frac{-Q}{r} + \frac{-QR\cos\theta}{2r^2} + \frac{-P\cos\theta}{r^2} + \frac{Q}{r'} + \frac{QR\cos\theta'}{2r'^2} + \frac{P\cos\theta'}{r'^2}\right] + Em(h + r\cos\theta) \quad (35)$$

$h>>r$, $h>>R$ *and* $r'>>r$, $\frac{1}{r'} \approx \frac{1}{2h}$ and neglect $\frac{P\cos\theta'}{r'^2}$ and $\frac{QR\cos\theta'}{2r^2}$ because of the r' term, hence Demanding $\emptyset(r,\theta) = 0$ *at* $r = R$ we get

$$\emptyset(r,\theta) = \frac{1}{4\pi\varepsilon_0}\left[\frac{-Q}{r} + \frac{-QR\cos\theta}{2r^2} + \frac{P\cos\theta}{r^2} + \frac{Q}{r'}\right] + Em(h + r\cos\theta) \quad (36)$$

$$0 = \frac{1}{4\pi\varepsilon_0}\left[\frac{-Q}{r} + \frac{-QR\cos\theta}{2r^2} + \frac{-P\cos\theta}{r^2} + \frac{Q}{r'} + \right] + Em(h + r\cos\theta) \quad (37)$$

$$Q = 4\pi\varepsilon 0EmhR(1 + \frac{R}{2h}) \quad (38)$$

$$P = 4\pi\varepsilon 0EmR^3 - 4\pi\varepsilon 0EmhR^2(1 + \frac{R}{2h}) \quad (39)$$

The Field strength at the top of the hemispherical CNT tip,

$$Eo = -\left[\frac{\partial(r, \theta = 0)}{\partial r}\right]_{r=R} \quad (40)$$

$$Eo = -\frac{2Q}{4\pi\varepsilon 0R^2} - \frac{2P}{4\pi\varepsilon 0R^3} - Em \quad (41)$$

$$Eo = -Em|\frac{h}{R} + 3.5| \quad (42)$$

We take effect of charges only and neglect the dipole moment under the assumption that distances between CNTs are quite large compared with their radius. Each nanotube tip will have charge $-Q$ and dipole moment $-P$ and their mirror image will have charge $+Q$ and dipole moment $+P$. We take the distance between the n^{th} CNT and the CNT under consideration as r_n[5] as shown in figure 3.8,

$$r_n = \sqrt{{x_n}^2 + {y_n}^2} \quad (43)$$

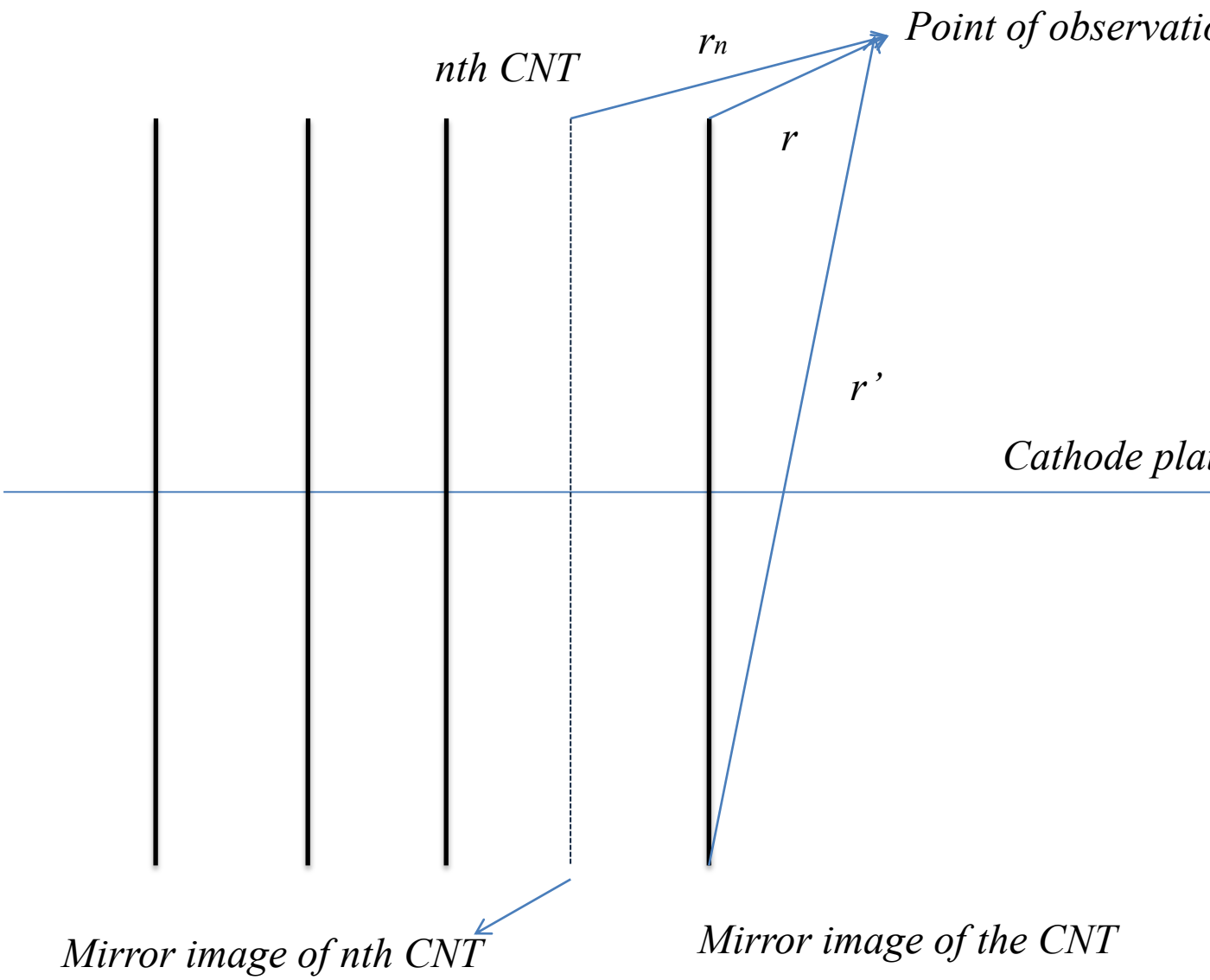

Figure 3. 8 Distribution of hemispherical CNT tips.

where $(x_n\ ,\ y_n)$ are the coordinates of the base of the CNTs w.r.t. the base of the CNT under consideration.

Demanding $\emptyset(r,\theta) = 0$ at r = R,

$$0 = \frac{1}{4\pi\varepsilon_0}\left[\frac{-Q}{r} + \frac{-QR\cos\theta}{2r^2} + \frac{-P\cos\theta}{r^2} + \frac{Q}{2h} + \sum_{n=1}^{m}\frac{-Q}{r_n} + \sum_{n=1}^{m}\frac{-QR\cos\theta}{2{r_n}^2} + \sum_{n=1}^{m}\frac{Q}{\sqrt{{r_n}^2 + (2h)^2}}\right] + Em(h + r\cos\theta) \quad (44)$$

$$Q = 4\pi\varepsilon_0 EmhR\left(1 + \frac{R}{2h} - \sum_{n=1}^{m}\frac{-R}{r_n} + \sum_{n=1}^{m}\frac{R}{\sqrt{{r_n}^2 + (2h)^2}}\right) \tag{45}$$

$$\begin{aligned} P = {} & 4\pi\varepsilon_0 EmR^3 - 4\pi\varepsilon_0 Emh\frac{R^2}{2}\left(1 + \frac{R}{2h} - \sum_{n=1}^{m}\frac{-R}{r_n} + \sum_{n=1}^{m}\frac{R}{\sqrt{{r_n}^2 + (2h)^2}}\right) \\ & - 4\pi\varepsilon_0 EmhR\left(1 + \frac{R}{2h} - \sum_{n=1}^{m}\frac{-R}{r_n} + \sum_{n=1}^{m}\frac{R}{\sqrt{{r_n}^2 + (2h)^2}}\right) \\ & \times\left(\sum_{n=1}^{m}\frac{-R^3}{2{r_n}^2}\right) \end{aligned} \tag{46}$$

The expression for field enhancement factor for the CNT array

$$\begin{aligned} \beta = \beta_0 - (& \sum_{n=1}^{m}\frac{h}{r_n} - \sum_{n=1}^{m}\frac{h}{\sqrt{{r_n}^2 + (2h)^2}} + 2Rh\sum_{n=1}^{m}\frac{1}{2{r_n}^2} + 2Rh\sum_{n=1}^{m}\frac{1}{2{r_n}^2}\times\frac{R}{2h} \\ & - 2Rh\sum_{n=1}^{m}\frac{R}{2{r_n}^3} + 2hR\sum_{n=1}^{m}\frac{R}{\sqrt{{r_n}^2 + (2h)^2}}\times\frac{R}{2{r_n}^2}) \end{aligned} \tag{47}$$

Let us assume the distance between the CNTs is s, then $r_n = s(a^2+b^2)^{\frac{1}{2}}$ where a and b are integers

$$\begin{aligned} \beta = \beta_0 - (& \sum_{a=0}^{m}\sum_{b=1}^{m}\frac{\frac{h}{s}}{(a^2+b^2)^{\frac{1}{2}}} - \sum_{a=0}^{m}\sum_{b=1}^{m}\frac{\frac{h}{s}}{\sqrt{a^2+b^2+\left(2\frac{h}{s}\right)^2}} \\ & + 2Rh\sum_{a=0}^{m}\sum_{b=1}^{m}\frac{1}{2s^2(a^2+b^2)} + 2Rh\sum_{a=0}^{m}\sum_{b=1}^{m}\frac{1}{2s^2(a^2+b^2)}\times\frac{R}{2h} \\ & - 2Rh\sum_{a=0}^{m}\sum_{b=1}^{m}\frac{R}{2s^3(a^2+b^2)^{\frac{3}{2}}} + 2hR\sum_{a=0}^{m}\sum_{b=1}^{m}\frac{R\frac{1}{s}}{\sqrt{a^2+b^2+\left(2\frac{h}{s}\right)^2}} \\ & \times\frac{R}{2{r_n}^2}) \end{aligned} \tag{48}$$

we can neglect terms with multiple of R(radius of the hemispherical CNT tip in nm) and h(length of the CNT in μm)$\approx 10^{-15}$

hence our required expression for field enhancement factor is

$$\beta = \beta_0 - \left(\sum_{n=1}^{m} \frac{\frac{h}{s}}{(a^2+b^2)^{\frac{1}{2}}} - \sum_{n=1}^{m} \frac{\frac{h}{s}}{\sqrt{a^2+b^2+\left(2\frac{h}{s}\right)^2}}\right) \quad (49)$$

hence we found that the expression of hemispherical CNT tip and the expression from considering floating spherical model of Ahmed et al[5] is same.

CHAPTER 4: Results and Conclusion

4.1. Results

4.1.1 Graph between Field enhancement factor and length of the hemispherical CNTs keeping spacing between CNTs constant i.e. s = 1μm and vary length of the CNTs upto 40 μm . As shown figure 4.1.

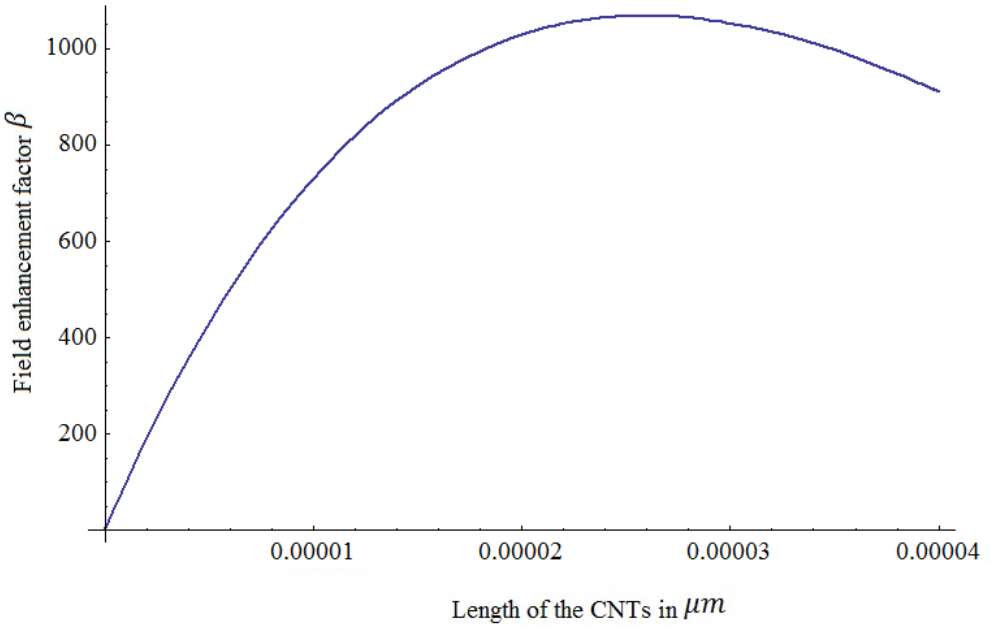

Figure 4.1 Field enhancement factor vs length of the CNT

In this plot the field enhancement factor increases due to increase in length of the CNT but decreases due to scanning effect which is also observed by Suh et al[17] and Ahmed et al[5].

4.1.2. Graph between Field enhancement factor and spacing between CNTs keeping length of the CNTs constant at $1\mu m$, and vary the spacing between CNTs upto 4 μm. As shown in figure 4.2.

In this plot we found that as we increase the distance between the CNT, the field enhancement factor first increases then become constant at certain value.

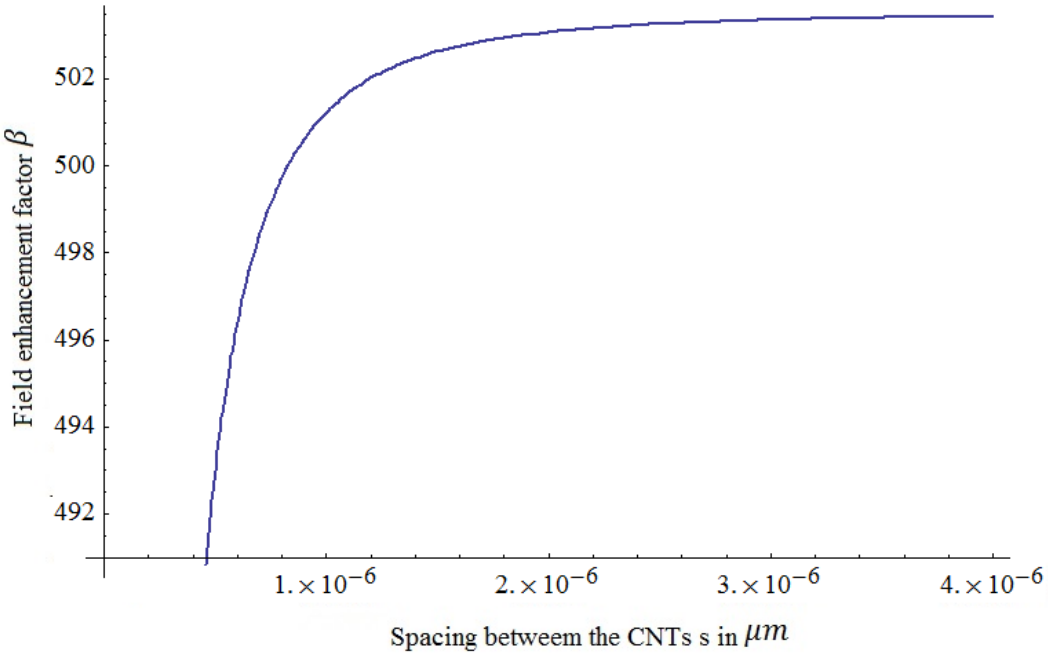

Figure 4.2 Field enhancement factor vs spacing 's' between the CNTs .

According to experimental result of Nilson et al[13]., the field emission from the densely

packed CNTs is poor because of the screening effect that reduces the field emission and the field emission for low density of CNTs are also poor because of insufficient space. In the intermediate the field emission is adequate.

We have compared our results with experimental results of Nilsson et al[13]. As show in figure 4.3

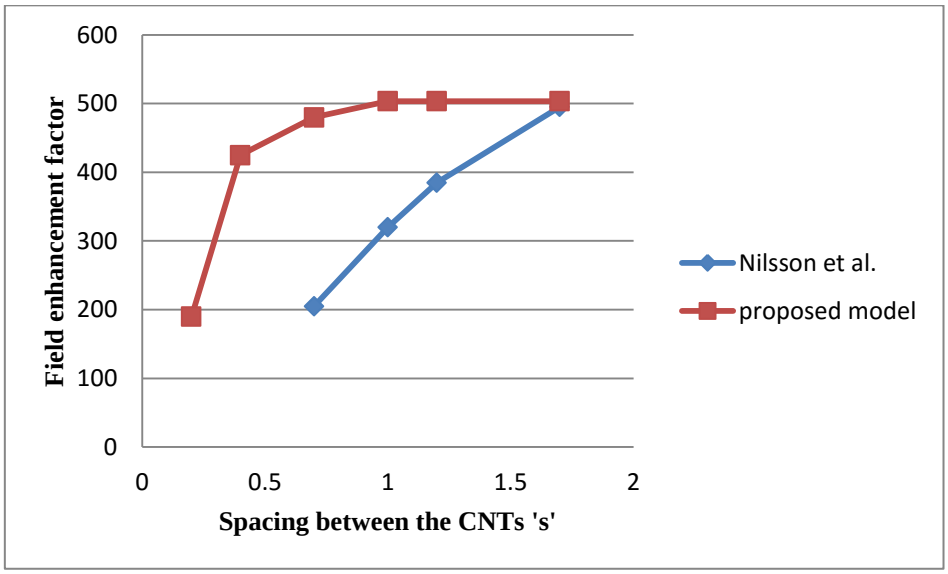

Figure 4.3 Field enhacement factor vs spacing 's' between CNTs Comparison of proposed model with experimental result of Nilson et al[13].

4.2 Conclusion

We have derived an expression of field enhancement factor for hemispherical CNT tip for any positional distribution of hemispherical CNT tip using mirror image method is more realistic than floating sphere model. we found that the field emission of hemispherical CNT tip is similar to the floating sphere[5]and the field emission of cluster of CNTs depend upon the length of the CNT and spacing between them. With increase in spacing between the hemispherical CNT the field enhancement factor first increases the become constant at certain value which similar to the theoretical result of Ahmed et al.[5] and with experimental results of Nilson et al.[13]. With increase in length of CNT the field enhancement factor is first increases then after certain it decreases this is because of the the electric scanned by neighbouring CNTs as Suh et al.[17] observed.

REFERENCES

[1] http://www.zyvex.com/nanotech/feynman.html.
[2] Introduction to nanoscience and technology, by K.K. Chattopadhyay and A.N. Banerjee.
[3] Grigory S. Bocharov and Alexander V. Eletskii, Nanomaterials 2013, 3, 393-442.
[4] D. Nicolaescu, J. Vac. Sci. Technol. B 11 (1993) 392.
[5] Amir Ahmad and V.K Tripathi, Institute of Physics Publishing ,Nanotechnology 17(2006) 3798-3801.
[6] T. Utsumi, IEEE Trans. Electron. Dev. ED-38 (1991) 2276.
[7] F. Rohrbach CERN Report 71-5/TC-L, 1971.
[8] G. Kokkoraskis, A. Modinos, J.P. Xanthalis, 47th International Field Emisiion Symposium, Berlin, July 2001(unpublished abstract).
[9] C.J. Edgcombe, U. Valdre, Solid State Electron. 45/6 (2001) 857.
[10] C.J. Edgcombe, U. Valdre, J. Microsc. 203 (2001) 188.
[11] R. G. Forbes, C.J. Edgcombe, U. Valdre, Ultramicroscopy 95 (2003) 57-65.
[12] Bonard J-M, Weiss N, Kind H, Tstokli T, Ferro L, Kern K and Chatelain A 2001 Adv. mater. (Weinheim, Ger.) 13 184.
[13] Nilson L, Groeing O, Emmenegger C, Kuettel O, Kuettel E, Schaller E, Schlabach L, Kind H, Bonard J M and Kern K 2000 Appl. phys. lett. 76 2071.
[14] X. Q. Wang, M. Wang, P. M. he and Y. B. XuJ. of Appl. Phys. vol. 96, numb. 11 (2004).
[15] Fredy R. Zypman, J. Phs. 74(4), April 2006.
[16] Indrek Mandre <indrek@mare.ee> htpp://www.mare.ee/indrek/
[17] Suh J S, Jeong K S, Jee J S and Han I 2002 Appl. Phys. Lett. 80 2392.
[18] X. Q. Wang, M. Wang, P. M. He, Y. B. Xu and Z. H. Li Journal of Applied Physics, Volume 96 Number 11
[19]X. Q. Wang, M. Wang, P. M. He, Y. B. Xu and Z H Li Ultramicroscopy 102(2005)181-187